

Deviations from planarity of copper-oxygen sheets in $\text{Ca}_{0.85}\text{Sr}_{0.15}\text{CuO}_2$

S. J. L. Billinge, P. K. Davies, and T. Egami

*Department of Materials Science and Engineering and Laboratory for Research on the Structure of Matter,
University of Pennsylvania, Philadelphia, Pennsylvania 19104-6272*

C. R. A. Catlow

Davey-Faraday Research Laboratories, Royal Institution, 21, Albemarle Street, London W1X 4BS, United Kingdom

(Received 16 October 1990; revised manuscript received 26 December 1990)

Deviations from perfect planarity of the copper-oxygen sheets in $\text{Ca}_{0.85}\text{Sr}_{0.15}\text{CuO}_2$ have been observed using pair-distribution-function analysis of pulsed-neutron-powder-diffraction data. These deviations take the form of displacements of oxygen atoms parallel to the z axis by 0.09 ± 0.02 Å at 10 K and 0.12 ± 0.04 Å at room temperature. The effect occurs on every oxygen site and may be correlated in sign from site to site, giving rise to short-range order. The average crystal structure, refined using Rietveld analysis, does not show this distortion, which must, therefore, extend only over short range. A lattice-energy-minimization calculation on the idealized compound CaCuO_2 , using pair potentials, indicates that such a distortion lowers the calculated lattice energy. A mechanism is proposed by which the strontium atoms break up the periodicity of the displacements and stabilize the structure.

I. INTRODUCTION

The single structural element common to all of the cuprate high- T_c superconductors is a plane made up of corner-sharing CuO_4 squares (hereafter referred to as the CuO_2 plane). This plane plays a key role in the normal-state conductivity and in the superconductivity of these materials.¹⁻⁶ The planes can occur singly, as in $\text{La}_{2-x}\text{M}_x\text{CuO}_4$ ($M = \text{Sr}, \text{Ba}, \text{Ca}$) (LA 2:1:4) (Ref. 7) and $\text{Tl}_2\text{Ba}_2\text{CuO}_6$ (TL 2:2:0:1),⁸ in pairs as in $\text{Tl}_2\text{Ba}_2\text{CaCu}_2\text{O}_8$ (TL 2:2:1:2) (Ref. 9) and $\text{YBa}_2\text{Cu}_3\text{O}_{(7-y)}$ (Y 1:2:3),^{10,11} or in stacks of three or more as in the family of compounds $A_2B_2\text{Ca}_{n-1}\text{Cu}_n\text{O}_{4+2n}$ ($A = \text{Tl}, \text{Bi}$ and $B = \text{Ba}, \text{Sr}$) (Ref. 12) for $n \geq 3$. These stacks can be thought of as defect perovskite blocks with $\frac{1}{3}$ of oxygen sites vacant in the positions between the CuO_2 planes. The blocks are separated from each other by intergrowth regions of distorted rocksaltlike structures. The idealized end member of the series $A_2B_2\text{Ca}_{n-1}\text{Cu}_n\text{O}_{4+2n}$ with $n \rightarrow \infty$ would have the formula CaCuO_2 and no intergrowth regions at all. Such a structure does form with the aid of 15% strontium substituted for calcium, although pure CaCuO_2 itself has a totally different structure.¹³ The resulting compound, $\text{Ca}_{0.85}\text{Sr}_{0.15}\text{CuO}_2$, can thus be considered to be the parent structure of the $A_2B_2\text{Ca}_{n-1}\text{Cu}_n\text{O}_{4+2n}$ family.

The CuO_2 sheets in the superconducting materials have been reported as being both truly planar, such as the central plane in TL 2:2:2:3,¹² or to be distorted as, for example, in La 2:1:4 (Refs. 7 and 14) and Y 1:2:3.¹¹ The sheets in $\text{Ca}_{0.85}\text{Sr}_{0.15}\text{CuO}_2$ are reported as being planar, however, the possibility that they may be distorted is not completely dismissed on the basis of an x-ray single-crystal study.¹³ Details of some of the structures of the planes in the different materials will be discussed later in the paper.

A common feature of all of the structural refinements

of the cuprate superconductors is the presence of large, anisotropic, thermal factors on certain sites. Rietveld refinements of the structures of the thallates indicate that large, "pancake-shaped," B factors are required on Tl and O(4) positions.^{8,9,12} These sites lie in the Tl-O layers which form part of the rocksalt intergrowths. Large thermal factors have also been refined on the lanthanum and apical oxygen O(2) sites in LA 2:1:4 compounds.¹⁴ These sites are also part of the intergrowth region in this material. Both large pancake^{15,16} and "cigar-shaped"¹⁷ thermal factors have been reported on the chain oxygen O(1) sites in Y 1:2:3. The cigars are oriented horizontally and perpendicular to the Cu—O—Cu bond. A large B factor, elongated along the z direction, on the apical O(4) oxygen site is also characteristic of refinements of this structure.^{11,15-17} A neutron-diffraction study showing the temperature dependence of the thermal factors in Y 1:2:3 (Ref. 11) indicates that the rms displacements on the O(1) chain site, in directions perpendicular to the Cu—O bond, decrease by 30–50% as the temperature falls from 300 to 75 K; however, they remain relatively invariant below that temperature down to 5 K. In general, a weak temperature dependence of thermal ellipsoids is observed. Similar behavior is seen in refinements of all the cuprate superconductor materials and large B factors persisting to low temperatures are widely reported. The reason is probably the presence of some static or quasistatic displacive disorder on these sites leading to a large uncertainty in atom position. Dmowski *et al.* have reported that a locally ordered structure with correlated rearrangements of thallium and oxygen is present in the Tl-O layers in Tl 2:2:1:2 using atom-pair distribution function (PDF) analysis of neutron-powder-diffraction data.¹⁸ Because the correlations do not extend over long distance and the order is short range only, it does not lead to any extra peaks in the diffraction profile and gives

a contribution only to the diffuse scattering. Diffraction profile refinements, which ignore the diffuse scattering, cannot extract this structural information and will just refine large B factors on these sites, as seen in the Rietveld analyses. When averaged over the whole crystal, this local order will appear just as an uncharacterized uncertainty in atom position.

Values for thermal factors on the copper and oxygen sites in the CuO_2 plane are also seen to be large and weakly temperature dependent. Mean-square displacements, $\langle u^2 \rangle$, up to $20 \times 10^{-3} \text{ \AA}^2$ are reported for oxygen in the z direction in Y 1:2:3 (Ref. 15) and up to $18 \times 10^{-3} \text{ \AA}^2$ in Tl 2:2:1:2. Similar thermal ellipsoids, elongated along the z direction, are reported on oxygen sites in La 2:1:4 (Ref. 14) and ellipsoids of similar magnitudes and shapes are also reported on copper sites on the CuO_2 plane in all these materials.

The purpose of the current work is to investigate the possibility that static or quasistatic atomic displacements, which would contribute to these large, weakly temperature-dependent, thermal ellipsoids, may be occurring in the CuO_2 plane sites. Displacements of ions occurring at these sites have been reported. Toby *et al.* have seen a structural change at T_c occurring to the CuO_2 planes in Tl 2:2:1:2 (Ref. 19) from PDF studies conducted over a range of temperatures. They attribute this to a change in the local ordering of atom displacements on the CuO_2 plane sites. Furthermore, the tetragonal-to-orthorhombic transition in La 2:1:4 can be attributed to a loss of correlation between planes of the atom displacements occurring in the CuO_2 planes of this material.²⁰

Since it is the intrinsic nature of the CuO_2 planes that is of interest in this work, the model compound $\text{Ca}_{0.85}\text{Sr}_{0.15}\text{CuO}_2$ has been chosen to be studied. Many of the results will be relevant to the planes in the superconducting materials and $\text{Ca}_{0.85}\text{Sr}_{0.15}\text{CuO}_2$ has the advantage that it has no intergrowth regions, which would complicate the structure of the planes. Anisotropic thermal factors up to $\langle u^2 \rangle = 9.7 \times 10^{-3}$ and $13 \times 10^{-3} \text{ \AA}^2$ have been reported on the copper and oxygen sites, respectively, in this material from an x-ray single-crystal refinement.¹³ These values are larger than expected from this structure as we discuss later, and are of similar magnitude to those refined on the equivalent sites in the superconducting structures even though there are no obvious structural elements that one would predict would disturb the planes. Either some uncharacterized static displacements of atoms, or else large-amplitude atomic oscillations must be present, even down to low temperature.

A technique able to probe local structures such as extended x-ray-absorption fine structure (EXAFS) or a PDF study of x-ray- or neutron-powder-diffraction data would be suitable to reveal such local structural information. The main technique used in the present study is the PDF analysis of pulsed neutron data. The pair distribution function has then been simulated from structural models to elicit the detailed structural information contained therein, and a quantitative least-squares minimization routine employed to refine structural parameters from the data. Since such a quantitative analysis of PDF's is a fairly new approach to crystal structure

refinement, the work will be described in some detail here. The structure has also been simulated with a lattice-energy-minimization technique using Born model potentials.

Using both theoretical and experimental methods, we find good evidence for a real static or quasistatic displacement of oxygen out of the CuO_2 plane which would lower the site symmetry for oxygen and copper from mmm (D_{2h}) to 2 (C_2). A model is proposed for this local structure. The modeling and the experimental results together suggest that there is probably a high degree of ionicity about the copper-oxygen bond. An ionic driving force for the displaced structure in $\text{Ca}_{0.85}\text{Sr}_{0.15}\text{CuO}_2$ is proposed and these findings are related to the superconducting cousins.

II. STRUCTURE OF $\text{Ca}_{0.85}\text{Sr}_{0.15}\text{CuO}_2$

The structure of $\text{Ca}_{0.85}\text{Sr}_{0.15}\text{CuO}_2$ has been refined from single-crystal x-ray-diffraction data yielding a primitive, tetragonal cell of space group $P4/mmm$ with $a=b=3.87611 \text{ \AA}$ and $c=3.1995 \text{ \AA}$.¹³ The structure is shown in Fig. 1. Alkaline-earth ions Ca^{2+} and Sr^{2+} separate the planes with about one in seven cells having strontium at its center. The presence of the strontium is required to stabilize the layered $\text{Ca}_{1-x}\text{Sr}_x\text{CuO}_2$ phase.²¹ Phase-equilibrium studies indicate that the range of solid solubility of strontium on calcium sites is very small, extending only from $x=0.13$ to 0.17 .²² There is no evidence that the Sr^{2+} is ordered over the calcium sites. Takano *et al.* have reported that the two-dimensional (2D) layered structure can be stabilized over a wider range of composition when the compound is formed un-

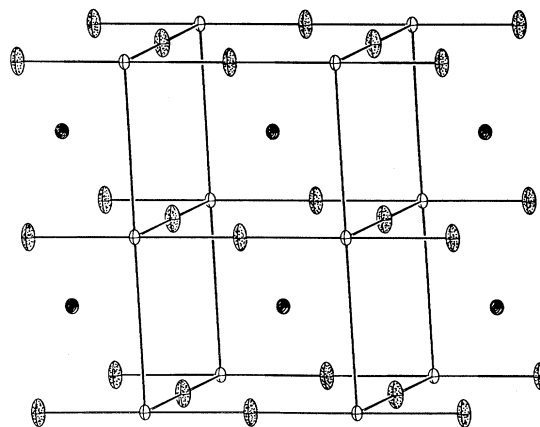


FIG. 1. Crystal structure of $\text{Ca}_{0.85}\text{Sr}_{0.15}\text{CuO}_2$ refined from neutron-powder-diffraction data. Oxygen sites are speckled and calcium-strontium sites are hatched. The ellipses represent thermal ellipsoids on the sites determined from anisotropic thermal factors refined from the PDF.

der increased pressures.²³ Compositions in the range $\text{Ca}_{0.33}\text{Sr}_{0.66}\text{CuO}_2$ to $\text{Ca}_{0.66}\text{Sr}_{0.33}\text{CuO}_2$ were stabilized for reactions taking place under 60 kbar pressure and 1050°C.

$\text{Ca}_{0.85}\text{Sr}_{0.15}\text{CuO}_2$ is an insulating antiferromagnet with spins of $\langle \mu \rangle = 0.51\mu_B$ per Cu atom lining up along $\langle 110 \rangle$ directions. Above the Néel temperature $T = 537$ K, the interplane spin-spin correlations are lost. However, the material remains a 2D Heisenberg antiferromagnet because of the strong intraplane interactions.²² This behavior is consistent with its being a Mott-Hubbard insulator.

III. PAIR-DISTRIBUTION-FUNCTION ANALYSIS

The atomic pair-distribution function is a representation of the distribution of interatomic distances present in a material. Traditionally its utility has been in analyzing scattering data from disordered materials such as glasses and liquids since the analysis presumes no periodicity. The procedure can, equally well, be applied to crystalline systems and PDF's of crystalline materials have been obtained with good accuracy.²⁴ The function can be produced from diffraction data by a Fourier transformation of the atom-atom interference function or total structure factor $S(Q)$. In detail,

$$\rho(r) = \rho_0 + \frac{1}{2\pi^2 r} \int_0^\infty Q[S(Q) - 1] \sin Qr \, dQ, \quad (1)$$

where $\rho(r)$ is the pair probability density, ρ_0 the mean density [corresponding to $\rho(r)$ as $r \rightarrow \infty$] and $Q = |\mathbf{Q}|$ is the scattering vector, $Q = 4\pi \sin\theta/\lambda$.²⁴

The function has proved to be very sensitive to local atomic displacements. It has also been able to differentiate successfully between random and short-range correlated atom displacements which often produce qualitative differences in the shapes of certain peaks in the function.^{18,20}

Although the function is simply a different representation of the reciprocal-space diffraction data, it is distinct from conventional crystallographic analyses in that all information in the diffraction pattern is utilized, including data out to very high Q (low d space) and all of the diffuse scattering. This is obviously important in totally disordered systems where the scattering is all diffuse, but it can also be important where a significant degree of non-periodic "disorder" is suspected in crystalline systems. Provided data is collected with good statistics out to high enough Q (which may be as much as 45 \AA^{-1} in a crystalline material at low T), then the PDF has shown itself to be quantitatively accurate.

In our experiments, neutron-powder diffraction data are collected using a time-of-flight spectrometer from a pulsed neutron source, with no energy discrimination at the detector. In such an energy dispersive experiment, both static and dynamic effects contribute to the scattering intensities and the structure refined is a superposition of instantaneous "snapshots" of the structure. Thus, it is not possible to distinguish whether observed disorder is fully static, quasistatic, or dynamic in nature from these experiments. A quasistatic atomic displacement occurs

on a site if the atomic potential is bifurcated allowing the atom to hop between the minima.

The raw data are normalized and corrected for background, absorption, multiple scattering and detector efficiency. A Placzek correction is applied to take account of inelastically scattered neutrons.²⁵ The total structure factor can then be reduced from the experimental total neutron differential cross section according to

$$S(Q) = \frac{1}{N \langle b \rangle^2} \left(\frac{d\sigma_c}{d\Omega} \right)_{\text{total}},$$

where N is the total number of scatterers and $\langle b \rangle^2$ are the squares of the scattering lengths averaged over the species of the sample.

Estimated statistical noise for points in the PDF are calculated by propagating errors derived from the counting statistics of the data.²⁶ Each point in the diffraction pattern is an independent observable and the estimated standard deviation (ESD) for each is simply \sqrt{N} for N counts. No smoothing is carried out during sample processing and the propagation thus provides an accurate estimate of ESD on each point in the PDF due to random errors. Systematic errors, however, will also contribute to the uncertainty in the PDF. Over the range of r from 2 to 10 Å, and provided the maximum Q measured is high enough, errors due to termination of the Fourier transform are small, as are errors introduced due to the instrument response function. Significant systematic errors are introduced by inadequate corrections for absorption, multiple scattering, source spectrum, and background but these are all slowly varying functions and lead to unacceptable uncertainties primarily in unphysical regions of the PDF where r is less than the nearest-neighbor distance. An estimate of their contribution to the total uncertainty in physical regions of the PDF has been made by carrying out a PDF analysis on a standard sample of Al.²⁶ They were found to be of the same order of magnitude as the random errors. The ESD's presented in this paper are from the random errors only and are provided as a guide to the reliability of the data. They will underestimate the total uncertainty but give an accurate assessment of the random errors. They vary smoothly with r being no more than 10% of ρ_0 at low r and much less over most of the PDF. Experimentally determined PDF's for the $\text{Ca}_{0.85}\text{Sr}_{0.15}\text{CuO}_2$ at the three temperatures are shown in Fig. 2, along with the ESD plotted as a function of r .

Structural information is extracted from the PDF by modeling using trial structures. The PDF of a model structure can be calculated by counting up all of the atom-atom vectors present in the crystal shorter than a cutoff r_{max} . These are plotted with δ functions at their ends on a scale in r . The δ functions are scaled by a factor which depends on the multiplicity of the vector and on the neutron-scattering strength of the atoms involved in the pair. Thermal motion of the atoms is simulated by convoluting the δ functions with normalized Gaussians.

To determine the goodness of fit between the simulated PDF and the experimentally derived one, an agreement factor (A -factor) is determined where

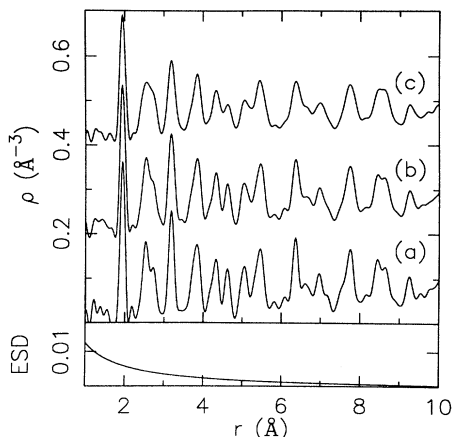


FIG. 2. Pair-distribution functions for $\text{Ca}_{0.85}\text{Sr}_{0.15}\text{CuO}_2$ at temperatures (a) 10 K, (b) 150 K, and (c) 298 K. The estimated standard deviation for points in the PDF due to random counting fluctuations are also plotted below with an enlarged scale.

$$A = \left[\frac{\int_{r_{\min}}^{r_{\max}} [\rho_{\text{dat}}(r) - \rho_{\text{sim}}(r; a_k)]^2 dr}{\int \rho_0^2 dr} \right]^{1/2},$$

$\rho_{\text{dat}}(r)$ is the value of the measured PDF and $\rho_{\text{sim}}(r; a_k)$ is the value of the simulated PDF at r . The latter is a function of parameters a_k . Least-squares minimizations of this function with respect to thermal factor parameters have been carried out to determine the model that gives the best agreement between its calculated PDF and data.

Modeling was accomplished using both isotropic and anisotropic thermal factors. Although the isotropic approximation is not a true indication of the real situation, it provides a reasonable first approximation and a good fit to data is possible on all but the peaks corresponding to nearest-neighbor pairs. An isotropic approximation has the advantage of simplifying the model considerably and reducing the number of fitting parameters to one per unique atom, for a given trial model. The Einstein approximation of independent harmonic motion of atoms is used in the modeling. This approximation is reasonable for non-nearest-neighbor pairs; however, including the nearest-neighbor peaks into the fitting will lead to incorrect values of the mean-square atomic displacements being refined. Nearest neighbors are directly bonded to each other and motion of the atoms in the pair is highly correlated which explains why these peaks are narrower than the model would predict. In the present analysis, simulated and measured PDF's were compared over the range from 2.9 to 10 Å to exclude the first three peaks which correspond to the nearest-neighbor distances between Cu—O, (Ca,Sr)—O, and O—O respectively.

A more complete modeling takes into account anisotropic atom motion. There are seven, symmetry-allowed, independent parameters that define thermal ellipsoids on the atom positions and these were used to determine the width of the Gaussian used for the convolution for each atom-atom pair.

IV. EXPERIMENT

Experiments were carried out on powdered samples. 36 g of $\text{Ca}_{0.85}\text{Sr}_{0.15}\text{CuO}_2$ were prepared by a solid-state reaction of CaCO_3 , SrCO_3 , and CuO . This mixture was decarbonated at 850 °C for 8 h, then baked at temperatures up to 980 °C for up to 60 h, with frequent grindings.

Neutron-powder-diffraction data were collected at the Intense Pulsed Neutron Source (IPNS) at Argonne National Laboratory using the time-of-flight, Special Environment Powder Diffractometer (SEPD).²⁷ 15 g of sample were sealed in a vanadium sample holder with He-exchange gas and cooled using a Displex closed-loop He refrigerator. Data were collected at 10, 150, and 298 K.

The data were subjected to both a Rietveld and a PDF analysis. The structure with the atoms constrained to their special positions was first considered. The modeling then proceeded systematically with the introduction of small atom displacements of $(\pm)\Delta$ from the high-symmetry positions. These atom positions were fixed and thermal factors were refined from both $S(Q)$ and PDF. The displacements were then increased step by step and the process repeated. Various possible displacements are suggested by the large B factors refined in the undistorted structure. Each of these was tried in the modeling. The distortions were (a) a shift of oxygen up and down parallel to z , (b) a shift of copper up and down parallel to z , (c) a shift of oxygen in plane along directions perpendicular to the Cu—O bond, and (d) a shift of oxygen parallel to $\langle 101 \rangle$ directions. The last distortion is suggested by the possibility of the disorder being some kind of lattice dilation to accommodate the oversize strontium ions.

The Rietveld refinements were carried out in the centrosymmetric space group $P4/mmm$ using the IPNS Rietveld package.²⁸ 122 reflections in the range $d=0.54\text{--}4.0$ Å were included. This space group constrains the oxygens to lie in the CuO_2 plane, or for the displacements to be randomly disordered. Initial refinements suggested that site occupancy was 100% and

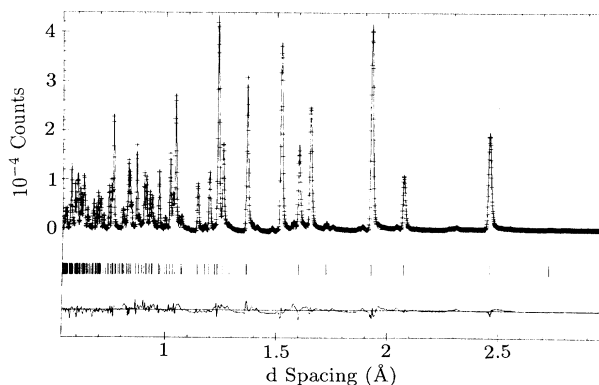


FIG. 3. An example of part of a Rietveld refinement for $\text{Ca}_{0.85}\text{Sr}_{0.15}\text{CuO}_2$ data taken at 10 K. Data are plotted as crosses. The solid line is the calculated profile. The tick marks below the profile indicate the positions of allowed diffraction peaks. A difference plot (observed-calculated) is shown at the bottom. The fitted background has been subtracted before plotting.

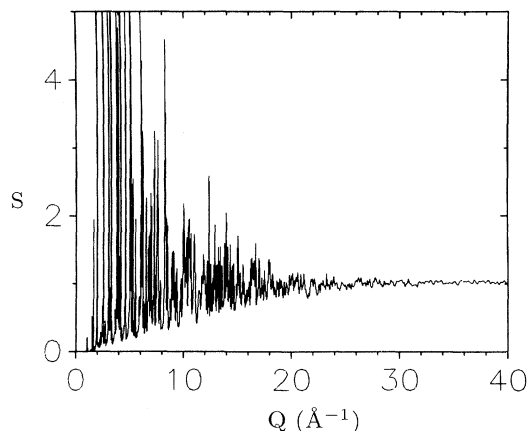


FIG. 4. Total structure factor $S(Q)$ for $\text{Ca}_{0.85}\text{Sr}_{0.15}\text{CuO}_2$ reduced from neutron-powder-diffraction data taken at 10 K. The structure in $S(Q)$ seen out to $Q=40 \text{ \AA}^{-1}$ is largely reproducible and is not due simply to statistical fluctuations.

this value was fixed on all sites. An example of a refinement on the 10-K data is shown in Fig. 3.

The PDF was calculated taking $S(Q)$ over a range of Q up to 40 \AA^{-1} ($d=0.157 \text{ \AA}$) with a mild damping applied between 25 and 40 \AA^{-1} . The $S(Q)$ from the 10-K data is shown in Fig. 4. The PDF's at the three temperatures

are shown in Fig. 2.

The results from the 10-K and 298-K refinements of $S(Q)$ and the PDF are presented in Table I. The Rietveld refined values for the undistorted structure at room temperature are of similar magnitude to those reported by Siegrist *et al.*¹³ However, the copper $\langle u_{33}^2 \rangle$ and the calcium-strontium $\langle u_{11}^2 \rangle$ values are higher, whereas the Ca-Sr $\langle u_{33}^2 \rangle$ is somewhat lower. The values refined from the PDF are in much better agreement with Siegrist *et al.*'s values though a much larger oxygen $\langle u_{33}^2 \rangle$ value was required in the current modeling. The PDF refined thermal factors are more physically reasonable than the Rietveld values from the same data, especially at low temperature, where negative thermal factors were consistently refined on copper sites and rather low values refined on other sites. These anomalous Rietveld values can be attributed to the pulsed neutron source itself which introduces an energy-dependent peak shape into the diffraction pattern which is significant at low neutron energies. This serves to suppress peak heights, though not integrated intensities, primarily in the low- Q region. The Rietveld analysis was performed over a relatively limited range of Q without a correction being made for the anomalous Q dependence of the peak shape. An improved analysis would require a more detailed determination of the instrument response function at the time of the experiment, which was not possible. In the real-space PDF, the thermal factors are determined from the widths of the Gaussian peaks which are insensitive to the details

TABLE I. Anisotropic thermal factors refined using Rietveld and pair-distribution-function fitting for the case of no oxygen displacements and for up and down displacements of $\Delta=0.1 \text{ \AA}$.

	Rietveld refined (10^{-3} \AA^2)			PDF refined (10^{-3} \AA^2)		
	$\langle u_{11}^2 \rangle$	$\langle u_{22}^2 \rangle$	$\langle u_{33}^2 \rangle$	$\langle u_{11}^2 \rangle$	$\langle u_{22}^2 \rangle$	$\langle u_{33}^2 \rangle$
10 K, $\Delta=0^a$						
Cu	-1.23	-1.23	1.78	2.91	2.91	3.76
Ca-Sr	3.93	3.93	3.29	3.11	3.11	0.86
O	1.08	3.23	8.40	2.13	4.57	16.6
10 K, $\Delta=0.10 \text{ \AA}^b$						
Cu	-1.15	-1.15	0.98	3.38	3.38	2.30
Ca-Sr	3.89	3.89	3.49	3.25	3.25	1.60
O	1.05	3.33	-1.63	1.76	3.72	8.28
298 K, $\Delta=0^{c,d}$						
Cu	2.01	2.01	12.39	3.64	3.64	7.81
Ca-Sr	9.85	9.85	5.64	5.51	5.51	8.10
O	3.20	8.66	18.47	5.58	7.40	26.80
298 K, $\Delta=0.10 \text{ \AA}^e$						
Cu	2.00	2.00	12.26	3.97	3.97	5.82
Ca-Sr	9.79	9.79	5.58	5.69	5.69	8.45
O	3.20	8.68	8.41	4.78	6.59	19.02

^aWeighted profile $R=0.11$, expected $R=0.02$, A factor = 0.14.

^b $R_w=0.11$, $R_e=0.02$, $A=0.13$.

^c $R_w=0.14$, $R_e=0.02$, $A=0.09$.

^dValues reported by Siegrist *et al.* are Cu: 2.7, 2.7, 9.7; Ca-Sr: 6.2, 6.2, 7.5; O: 4.6, 8.8, 13.0. (10^{-3} \AA^2). Reference 13.

^e $R_w=0.14$, $R_e=0.02$, $A=0.09$.

of the diffraction peak shapes and, furthermore, originate in the high- Q region of $S(Q)$ where the anomalous energy-dependent peak-shape problem is not significant. Thus, even though these Rietveld refined thermal factors are unreasonable, those refined from the PDF should give a reliable indication of real atomic motion.

Atomic displacements were introduced into the simulated structure maintaining isotropic thermal factors on each site. Both random displacements and displacements correlated from site to site were tried. Although no nuclear superlattice peaks have been reported, local correlations which do not give rise to periodic superstructures are still a possibility and a number of such models were considered. The high symmetry of the unit cell meant that the PDF's of cell-doubling models with correlated atom displacements could not be distinguished from each other or from the randomly displaced case and modeling proceeded using displacements which were random from cell to cell. The results from the PDF refinements for the case of oxygen displacing along the z direction (O_z) are shown in Fig. 5. For each fixed value of Δ , isotropic thermal factors were refined to minimize the A factor and it is these "best-fit" values of agreement factor that are plotted. It was seen that the best-fit A factor diverged very quickly ($\Delta < 0.06 \text{ \AA}$) for all of the distortions tried except for the O_z displacements. In the latter case the curve fell to a minimum before finally diverging at significant values of Δ . This indicates that all the distortions introduce peak shifts into the simulated PDF which cannot be reconciled with the experimentally determined PDF; except for the O_z case. Thus, the evidence discounts the possibility of all but the O_z distortion existing up to any significant value of Δ . The most likely magnitude to assign to the oxygen displacement would be the value where the best-fit A factor versus the Δ curve has a minimum. The curves have somewhat broad minima; however, it is clear that any real atomic displacement cannot be larger than the value of Δ at which the best-fit A factor diverges. Thus, from Fig. 5, the displacements

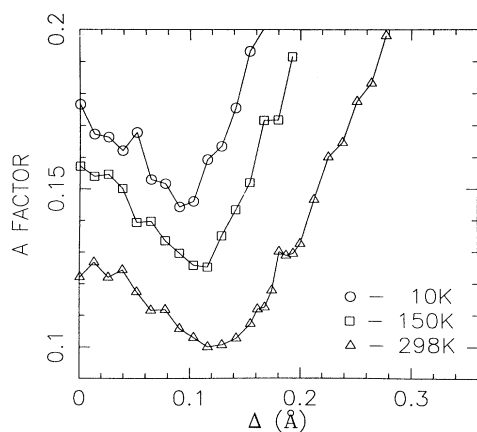


FIG. 5. Plots of the best-fit agreement factors vs displacement, where oxygens are displacing up and down along z by $\pm\Delta$. This A factor is the agreement between a simulated PDF and the experimentally derived one, after refining isotropic thermal factors on each site.

above and below the plane can take magnitudes $0.09 \pm 0.02 \text{ \AA}$ at 10 K, $0.10 \pm 0.03 \text{ \AA}$ at 150 K, and $0.12 \pm 0.04 \text{ \AA}$ at room temperature.

A similar procedure was applied in the Rietveld analysis and the best-fit weighted profile R factors, as a function of Δ , are shown in Fig. 6. The curves are flatter and diverge more slowly than the A -factor curves and show no clear minimum. Their general behavior, however, is consistent with that of the A factor, diverging for $\Delta > 0.12 \text{ \AA}$. The Rietveld analysis thus does not deny the possibility of the existence of the O_z distortion. However, it does not provide definite evidence in support of such a conclusion.

This material is highly anisotropic in nature and so it is important to take account of anisotropic motions of atoms in the modeling to gain a more realistic picture of the crystal. The results from the 10-K data involving anisotropic thermal factors are shown in Fig. 7. The lower curve shows the variation in the best-fit A factor with increasing oxygen displacement. Because of the larger number of fitting parameters, the A factor is smaller and has no clear minimum but has a plateau which extends to $\Delta = 0.1 \text{ \AA}$ before diverging sharply. As with the analysis using isotropic thermal factors, we see that a displacement of oxygen greater than $\pm 0.11 \text{ \AA}$ out of the plane is incompatible with the measured PDF. The upper curve indicates the corresponding refined mean-square displacements of oxygen, also along the z direction, for each displacement. For $\Delta \leq 0.04 \text{ \AA}$ a good fit is possible, of simulated PDF to data, for a large value of $\langle u_{33}^{22} \rangle$ of $16.6 \times 10^{-3} \text{ \AA}^2$ on the oxygen site. For $\Delta > 0.04 \text{ \AA}$, the best fit is obtained for much lower $\langle u_{33}^{22} \rangle$ values, the minimum value being $\langle u_{33}^{22} \rangle = 8.5 \times 10^{-3} \text{ \AA}^2$ for $\Delta = 0.1 \text{ \AA}$. The physical appropriateness of these values will be discussed later.

A similar procedure was used in the Rietveld analysis. As in the isotropic case, the R factor was less sensitive to the introduction of the displacements than the A factor.

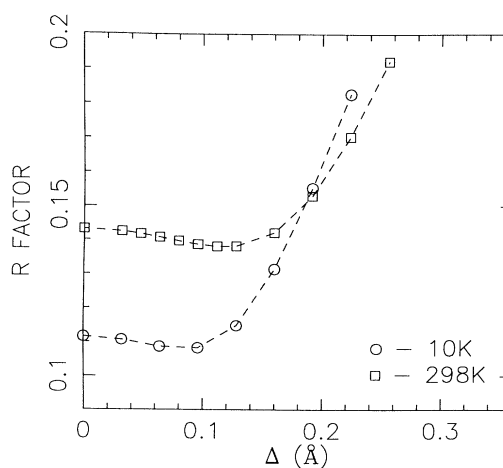


FIG. 6. Plots of the best-fit Rietveld refined weighted profile R factors vs displacement of oxygen up and down along z by $\pm\Delta$ for the case of isotropic thermal factors on each atom site. This figure can be compared with Fig. 5, where the agreement factors are from a fit of the pair-distribution function for the same data.

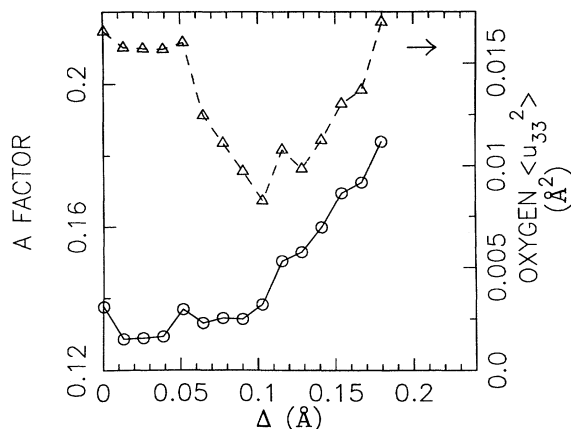


FIG. 7. Plot of best-fit agreement factors (circles) vs oxygen displacements along z for modeling using anisotropic thermal factors on data taken at 10 K. Also shown is the corresponding plot of oxygen mean-square displacement in the z direction $\langle u_{33}^2 \rangle$ (triangles). Values were refined from the PDF.

It only varied in the fourth significant figure until it diverged, more slowly than the A factor, for $\Delta \geq 0.132$ Å in the case of the O_z displacement. The thermal factors changed little with Δ except for the oxygen $\langle u_{33}^2 \rangle$ value which fell sharply and took negative values for $\Delta > 0.08$ Å. This might signify the limit of physically justifiable behavior, though, as discussed before, the thermal factors are somewhat low and the values refined from the PDF are probably more reliable.

Two possible situations can be considered therefore. One is the case of there being no distortion to the planes but a large, anisotropic and truly dynamic thermal factor. The other possibility is that a static, or quasistatic, displacement of oxygen exists of magnitude 0.1 Å with smaller thermal factors on the displaced sites. The PDF results provide the best evidence for deciding which is more likely. The same anisotropic B -factor analysis as has been described for the 10-K data was carried out on data taken at 150 and 298 K. The expected temperature dependence of $\langle u^2 \rangle$ can be estimated using Debye theory. From the anisotropic thermal factors for the oxygen site, refined from the PDF, an average isotropic value was calculated for the cases of (a) no distortion and (b) the O_z distortion with $\Delta = 0.1$ Å at each temperature. These measured values are plotted as circles and asterisks, respectively in Fig. 8, as a function of temperature. In the two cases, a Debye temperature for the oxygen site was determined by fitting the 10-K data point, and then the expected temperature dependence of $\langle u^2 \rangle$ corresponding to this Debye temperature was plotted according to the relationship

$$\langle u^2 \rangle = \frac{3h^2}{4\pi^2 m k_B \Theta_D} \left[\frac{\phi(\Theta_D/T)}{\Theta_D/T} + \frac{1}{4} \right],$$

where k_B is the Boltzmann constant, m is the atomic mass in kg, Θ_D is the Debye temperature, and T is the

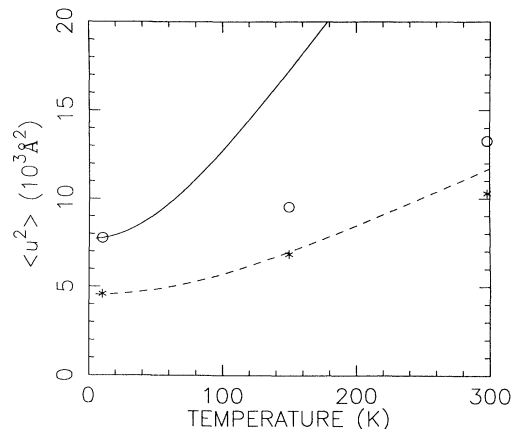


FIG. 8. Temperature dependence of oxygen thermal factors. Circles are values refined from the PDF assuming no oxygen displacements, asterisks are values refined assuming 0.1 Å displacements along z . The lines indicate the expected temperature dependence from Debye theory if the 10 K data point is fitted in each case.

temperature. The Debye integral function is given by

$$\phi(x) = \left[\frac{1}{x} \right] \int_0^x \left\{ \frac{\xi}{\exp(\xi) - 1} \right\} d\xi.$$

Debye theory is strictly applicable to isotropic, monatomic lattices only. In the present case it has been applied to the isotropically averaged vibrations of the oxygen sublattice. This is reasonable as a first approximation, especially since values are being compared in a low-temperature region. In this region, only the low-frequency modes will be excited originating in the part of the phonon spectrum which is closest in form to the ideal Debye spectrum.

The Debye temperature determined for the case of displaced oxygen atoms is $\Theta_D = 500$ K, and this predicts a temperature variation of $\langle u^2 \rangle$ very close to that observed in experiment. The zero-point motion which would be necessary to explain the temperature factor refined when no oxygen displacement is assumed requires a Debye temperature of $\Theta_D = 295$ K. The predicted temperature dependence of such a motion is much stronger than that observed, as is evident in Fig. 8, and would lead to a room-temperature thermal factor three times larger than that observed. The low-temperature vibrations are, thus, much better explained when a static, or quasistatic, displacement of oxygen of $\Delta = 0.1$ Å is assumed on those sites.

To summarize, the fact that the best-fit A -factor curves do not diverge immediately on introducing a displacement of oxygen along z and, in the isotropic analysis, actually fall to a minimum value, indicates that a static displacement of O is possible from consideration of the PDF. This behavior was not shown in similar analyses when the other distortions were considered which indicates that this kind of analysis is sensitive to such small distortions. Further evidence is the values of thermal

factors which, when refined from the PDF with the distortion assumed in the modeling, have values that are more consistent with physical models of lattice vibrations. It should be noted that, as discussed earlier, it is not possible to ascertain whether the displacements are fully static or are quasistatic and discussion of a "static" displacement does not rule out the possibility that it is, in fact, a dynamic feature of the structure involving atoms hopping between displaced local minima in the potential.

V. LATTICE-ENERGY MINIMIZATION CALCULATION

In contrast to the superconducting cuprates, there are no obvious crystal chemical features of the structure of $\text{Ca}_{0.85}\text{Sr}_{0.15}\text{CuO}_2$ that would lead to a displacement of the oxygen atoms. The PDF modeling indicates that distortions are present on all of the oxygen sites which would suggest that the driving force is something other than simply an accommodation of the oversized strontium ions in every seventh cell, although, clearly these ions are necessary to stabilize the structure.

In order to investigate a possible driving force for the displacements and to look into the nature of the strontium substitutions and the relaxation of the lattice around strontium ions, lattice-energy calculations have been carried out. An ionic model was used with two-body central-force pair potentials of the Buckingham form with the shell model of Dick and Overhauser²⁹ used to describe polarizability. The form of the pair potentials and the polarizabilities (α) are shown below:

$$V(r) = A \exp \left[\frac{-r}{\rho} \right] - \frac{C}{r^6},$$

$$\alpha = \frac{Y^2}{k}.$$

A , ρ , C , Y , and k are empirically determined parameters. Y is the charge contained in the massless shell, corresponding to an effective valence charge, and k is the harmonic spring constant connecting the shell to the core. No data are available for the elastic or dielectric constants of $\text{Ca}_{0.85}\text{Sr}_{0.15}\text{CuO}_2$ and so the parameters were determined using data from CuO , CaO and SrO (Ref. 30) and transferred. The same potential parameters have

been used successfully to model other layered copper-oxide compounds^{31,32} although three-body bond-bending terms were required to describe the distortions of the CuO_6 octahedra present in those structures. In the present case, to maintain simplicity, no bond-bending terms were included. The distorted octahedra are not present in $\text{Ca}_{0.85}\text{Sr}_{0.15}\text{CuO}_2$ and so it is not clear how important such terms would be. A more refined model might include an $\text{O}(1)\text{-Cu-O}(1)$ bending term. The validity of the potentials used was assessed by their success in reproducing the observed atom positions and unit-cell dimensions. A final check was made by comparison of a calculated and measured phonon density of states, as will be discussed later. The assumption of pure ionicity is clearly not an accurate one since this material exhibits a degree of covalency, especially in the CuO_2 plane. Thus, the calculations are not necessarily expected to be quantitatively predictive. However, this compound does have significant ionic character. Furthermore, lattice-energy calculations have been used successfully even for systems with a considerable covalent character such as in the family of silicates; α -quartz, MgSiO_3 perovskite, zeolites, and even vitreous silica.³³⁻³⁶ The values of all the potential parameters used are given in Table II. The lattice energy was minimized with respect to variations in atomic coordinates, maintaining constant volume (lattice constants constrained). The resulting atomic coordinates are given in Table III and the static dielectric constants, elastic constants, and lattice energies are given in Table IV.

Interestingly, these calculations showed that the introduction of an O_z -type displacement had the effect of lowering the lattice energy by a small amount. Indeed, an energy minimum was found when oxygen was displaced along z by 0.3 Å. Initial calculations were carried out assuming no strontium content and a formula CaCuO_2 , forming the layered structure of $\text{Ca}_{0.85}\text{Sr}_{0.15}\text{CuO}_2$. The potentials used predicted a lattice energy of -74.253 eV/formula unit. The calculated elastic constants appeared reasonable, although direct comparison is not possible as these data are not available for $\text{Ca}_{0.85}\text{Sr}_{0.15}\text{CuO}_2$. The unit cell was fixed with $a=b=3.8611$ Å and $c=3.1995$ Å and the potentials fitted well with that constraint, so that only a small residual bulk lattice stress, equivalent to a strain of no more than 0.017, was calculated. Thus, even though the poten-

TABLE II. Potential parameters and shell constants for the computer simulation calculation.

	Buckingham potential (potential cutoff=4 Å)		
	A (eV)	ρ (Å)	C (eV Å ⁻¹)
$\text{Cu}^{2+}\text{—O}^{2-}$	294.15	0.400 23	0.0
$\text{O}^{2-}\text{—O}^{2-}$	22 764.3	0.149	43.0
$\text{Ca}^{2+}\text{—O}^{2-}$	1 228.9	0.337 2	0.0
$\text{Sr}^{2+}\text{—O}^{2-}$	959.1	0.372 1	0.0
	Shell model		
	$Y(e)$	k (eV Å ⁻²)	
Cu^{2+}	+1.09	10 ⁵	
O^{2-}	-2.389	42.0	

TABLE III. Atomic coordinates obtained from the simulation after lattice-energy minimization. The lattice constants used were $a = b = 3.8611 \text{ \AA}$ and $c = 3.1995 \text{ \AA}$.

	x	y	z
Cu	0.0000	0.0000	0.0000
Ca-Sr	0.5000	0.5000	0.5000
O	0.0000	0.5000	0.0999
O	0.5000	0.0000	0.9001

tials were transferred from other materials, they still predict the same unit-cell size here to within 2%. As a further check on the validity of the potentials, a phonon density of states was calculated for the simulated material and compared with one determined experimentally using inelastic neutron scattering from the Low Resolution Medium Energy Chopper Spectrometer (LRMECS) at the IPNS. The agreement was good, with a broad peak around 30-meV energy transfer and another peak close to 50 meV. The experimental single phonon intensity disappeared around 80 meV. In the simulated density of states, the final peak had its maximum around 10 meV lower than the experimental case, but also fell to zero at 80 meV. The energy resolution in the experiment was around 6-meV energy transfer. The good agreement thus inspires some confidence in the ability of these potentials to describe behavior in this solid.

We should note that a negative value for the static dielectric constant ϵ_{11} shows that the material is unstable with respect to a ferroelectric type of distortion, which might be expected in such a defect perovskite structure. Furthermore, the calculated phonon dispersion curves had three imaginary branches indicating that the structure is unstable with respect to certain lattice distortions. Both of these problems were mitigated, but not totally solved by the introduction of the O_z displacement. The dielectric constants became less negative and only one branch of the dispersion curve remained wholly imaginary. The other possible distortions that were considered in the PDF modeling were also tried in the simulation but each one produced an increase in lattice energy.

The O_z displacement introduced a large compressive

stress along the z direction which, if allowed to relax, would produce a 10% strain in that direction. When the lattice parameters were allowed to relax to release this elastic energy, a totally new tetragonal structure was predicted with a long c parameter and a reduced a and b dimension. Such a relaxation does not occur in the real material.

The identical structure, but with Sr^{2+} completely substituted for all the Ca^{2+} ions, was then studied. Again, this had a negative lattice energy and negative static dielectric constant ϵ_{11} values. Introducing O_z -type distortions in the present case, however, raised the lattice energy which indicates that the ordered O_z displacements are not preferred around strontium ions. As before, imposing an O_z distortion of magnitude 0.3 \AA introduced a lattice pressure along the z direction. However, when this was allowed to relax, it did so with no reduction in the a - b dimension of the cell. Thus, it appears that the presence of strontium ions would impede such a compression of a and b in the mixed $Ca_{0.85}Sr_{0.15}CuO_2$ structure. Furthermore, the strontium ions will oppose the occurrence of the O_z distortion in their neighborhood and thus would break up the long-range periodicity of the oxygen displacements. This would have the effect of lowering the internal stress associated with the distortion and limiting it to being a short-range phenomenon. Together these two effects produce a mechanism by which the presence of strontium could stabilize this structure.

The relaxation of the lattice around a Sr^{2+} ion was also studied because it has been suggested that this may be the source of the disorder observed in crystallographic analyses.¹³ Strontium was introduced into the pure $CaCuO_2$ model in two ways. To model the case of an even distribution of isolated strontium ions throughout the lattice, an eight-cell supercell was constructed and Sr^{2+} substituted onto one of the calcium sites. This was then used as the unit cell in a perfect lattice calculation and the lattice energy minimized with respect to local atom reorganizations. This model implies a perfect, long-range substitutional order of strontium on calcium sites which has not been observed experimentally. However, it is a good approximation for an even distribution of isolated strontium ions. The relaxed structure had a lattice energy of $-73.865 \text{ eV/formula unit}$ corresponding to an increase

TABLE IV. Properties calculated for the idealized $CaCuO_2$ structure with undistorted CuO_2 planes and oxygen displaced along z by 0.3 \AA .

		Undistorted	Distorted structure	
Lattice energy		-74.253	-74.430	eV/Formula unit
Static dielectric constant	ϵ_{11}	-34.98	-17.75	
	ϵ_{33}	10.257	10.034	
Elastic constants	c_{11}	28.607	15.928	$10^{11} \text{ dyn cm}^{-2}$
	c_{33}	29.282	11.339	
	c_{44}	3.204	4.0125	
	c_{66}	21.601	20.188	
	c_{14}	27.134	23.048	
	c_{13}	2.436	4.039	

in energy of 0.388 eV/formula unit for the introduction of the strontium ion.

The presence of strontium was also modeled by introducing a single Sr^{2+} ion on a calcium site as an isolated point defect. A defect energy calculation was carried out using the Mott-Littleton approach.^{37,38} This gave a defect energy of 0.304 eV. Both of these results indicate that the degree of atomic reorganization required to accommodate the strontium ion is small. The closest oxygen and copper ions to the defect moved by, at most, 0.06 Å and the displacements of ions situated beyond this were an order of magnitude less. Thus, this accommodation is very localized to the strontium and would affect, at most, no more than half of the oxygen and copper atoms. Furthermore, the relaxation predicted some motion of oxygen along the x and y directions, and also some displacements of copper of between 0.04 and 0.06 Å. Significant atom displacements in these directions were not seen in the PDF. The implication therefore is that the distortions observed experimentally are not explained simply by the presence of 15% of misfit strontium ions on calcium sites.

VI. DISCUSSION

A. CuO_2 plane in superconducting compounds

The occurrence of CuO_2 planes in the superconducting cuprates can be categorized into three distinct groups. CuO_2 sheets occurring singly have Cu(II) in a (4+2) distorted octahedral coordination with apical oxygens above and below each copper at a distance of around 2.4–2.7 Å, compared to the copper-oxygen separation in the plane of around 1.9 Å. The apical oxygens are much less tightly bonded to the copper and also form a part of the intergrowth rocksalt layer above. Examples of this type are the LA 2:1:4 (Ref. 14) structures and $\text{Tl}_2\text{Ba}_2\text{CuO}_6$.⁸ The next group is that categorized by compounds containing paired CuO_2 sheets. In this case the sheets are separated by an alkaline-earth ion or, in the case of Y 1:2:3, by yttrium, and the copper is in a (4+1) coordination surrounded by oxygen in a square pyramidal configuration. Again, the apical oxygen is at a larger separation from copper than the in-plane oxygen atoms and there are no oxygen atoms between the planes, which are separated by a distance of about 3.2 Å. Examples of this class of CuO_2 plane are those in Y 1:2:3 (Ref. 11) and Tl 2:2:1:2.⁹ The final category is that of planes that are sandwiched between other planes, for instance, the middle planes in the $A_2B_2\text{Ca}_{n-1}\text{Cu}_n\text{O}_{4+2n}$ ($A = \text{Tl, Bi}$ and $B = \text{Ba, Sr}$) family of compounds for $n \geq 3$.¹² In this family of compounds, n determines the number of CuO_2 planes which stack together consecutively in the perovskite blocks. Thus $n = 3$ indicates that there will be three planes stacked up; one central plane of the third category between two others from the second category. The planes of the compound $\text{Ca}_{0.85}\text{Sr}_{0.15}\text{CuO}_2$ belong to the third category. The reason for categorizing the planes by their environment in this way is to help in extrapolating results back from the model compound to the more interesting cases of the superconducting materials. Planes in category three have

identical environments to the $\text{Ca}_{0.85}\text{Sr}_{0.15}\text{CuO}_2$ and we might expect a close resemblance of the behavior in each. Although the environments of category one and two planes are different, certain of the results from the model structure will also be relevant to these planes. The apical oxygens are only loosely bonded to the copper and the planes remain essentially two dimensional as in the model compound, although, clearly the effects of other structural elements will dictate the precise character of these planes.

B. CuO_2 plane in $\text{Ca}_{0.85}\text{Sr}_{0.15}\text{CuO}_2$

The large but weakly temperature-dependent thermal factors that were refined from the PDF analysis, especially on the copper and oxygen sites, are an indication that some degree of disordering is present on those sites. There is nothing self-evident in the structure which might explain this other than the idea that an uncertainty in atom position may be produced by relaxation around misfit Sr^{2+} ions which sit in every seventh unit cell. Lattice calculations indicate that in fact this makes only a small contribution to the observed disorder. PDF modeling was able to characterize the disorder as a displacement of oxygen up and down along the z direction occurring on every oxygen site, of up to 0.12 Å in magnitude at room temperature. It was not able to determine whether this occurred in a correlated fashion or randomly from site to site. PDF analysis is normally very sensitive to this distinction. However, in the present case, the high symmetry of this system means that both correlated and disordered models produce almost identical atom-atom correlations and thus an indistinguishable PDF. The direction and magnitude of the ion displacements does, however, make significant changes to the PDF. Although it is not possible to prove a correlated model, neither should it be discounted and intuition and precedent might lend one to suppose that atom displacements are correlated in some way. The distinction is important for determining point symmetries of the atom sites and so deserves some consideration. There is known to be direct O-O bonding across the cell corner, as well as indirectly through the copper, and so a direct link exists from one CuO_4 square plate to an adjacent one which would suggest some dialogue between displaced oxygens. Furthermore, the lattice-energy-minimization calculations, which predicted a lattice-energy minimum for 0.3 Å displacements of oxygen, using a correlated model, oxygen displacing up and down on alternating sites. Correlated oxygen displacements have also been reported in the CuO_2 planes of Tl 2:2:1:2 by Toby *et al.*¹⁹ An orthorhombic type of correlated distortion, similar to the distortion in La 2:1:4 (Ref. 7) and the $\langle 110 \rangle$ model of Toby¹⁹ was used during the PDF modeling and is shown in Fig. 9. An undistorted oxygen has site symmetry mmm (D_{2h}). A random distortion, on average, leaves this unchanged. However, if the distortion is the orthorhombic correlated model presented in this paper, the oxygen site symmetry is lowered to 2 (C_2).

The fact that our calculations have modeled the distortion suggests that its origin can be understood in terms of simple potential models based on central force fields. We

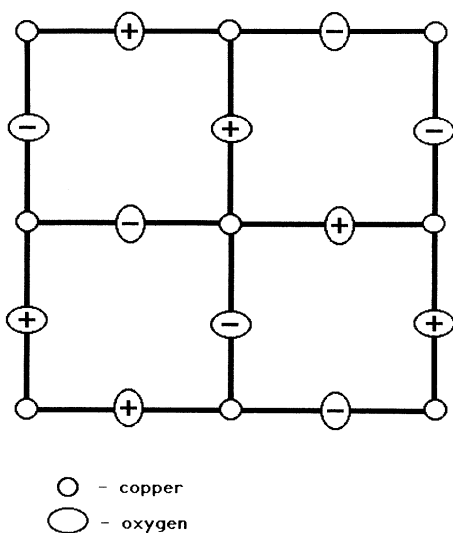


FIG. 9. The pattern of correlated displacements of oxygen which was used in the modeling. Pluses indicate a displacement of Δ up from the plane and minuses indicate a movement downwards. This is one of a number of possible patterns of correlations which produced PDF's that could not be distinguished within the ESD over the range $r < 10 \text{ \AA}$.

consider the origin may be the unusually long Ca-O bond. Using ionic radius data, the ideal Ca-O distance is calculated to be 2.47 (Ref. 39) and the distance in the crystal is 2.51 \AA . If the shape of the crystal potential is convex in this region then a splitting of the bonds to become equally longer and shorter would produce an overall saving in energy since the shorter bonds would gain a greater saving in energy than the longer bonds would lose. For a value of $\Delta = 0.1 \text{ \AA}$ the short Ca-O bond becomes 2.44 \AA and the long bond becomes 2.57 \AA , placing the shorter bond close to the ideal Ca-O ionic separation. This can also be thought of in terms of bond-valence theory.⁴⁰ This empirical theory uses the bond valence in ionic structures defined as the integral cationic valence divided by its coordination number. Thus, for Ca^{2+} in $\text{Ca}_{0.85}\text{Sr}_{0.15}\text{CuO}_2$ in eightfold coordination the average bond valence will be 0.25 valence units. The predictive value of the theory comes from the close correlation of a particular bond valence with the observed bond length. The relationship can be expressed as $s = (R/R_0)^{-N}$,⁴⁰ where s is the bond valence, R is the bond length, R_0 and N are empirically derived parameters, R_0 corresponding to the bond length for unit valence. The nonlinearity of this relationship has been used to predict the occurrence of distortions in situations where ions cannot take up their ideal bond length, since a lengthening and shortening of bonds will increase the average bond valence. This theory has been able to predict distortions occurring in ABX_3 perovskite structures in good agreement with observations.⁴¹ In the present case the undistorted bond length $R = 2.51 \text{ \AA}$ gives $s = 0.230$ valence units, somewhat lower than the expected value. If the oxygens dis-

place up and down by 0.3 \AA then there are four bonds of length $R = 2.33 \text{ \AA}$, $s = 0.341$, and four bonds of $R = 2.71 \text{ \AA}$, $s = 0.151$ valence units, thus the average bond valence is raised, simply by introducing the distortion, to 0.246 valence units. The real distortion is closer to $\Delta = 0.1 \text{ \AA}$, however, this still raises the average bond valence towards the ideal value.

The computer simulation indicated some interesting consequences of the existence of the distortion and it is worthwhile to speculate on their importance. We should note, however, that values of dielectric and elastic constants have not been measured on this material to compare with the calculated values, so the accuracy of the potentials has not been verified. The great utility of computer calculations, however, is that they give an indication of the fundamentals behind observed properties and can help to give greater insight into a physical system. There are four noteworthy results which will be considered under the groupings of ferroelectric behavior, lattice pressure, elastic constants, and the role of strontium.

The fact that the model structure is unstable with respect to a ferroelectric distortion is indicated by the presence of negative static dielectric constants (Table IV). That the structure is unstable with respect to some atomic rearrangements is also borne out by the existence of imaginary branches in the phonon dispersion relations. Introduction of the O_z distortion makes the dielectric constants less negative, i.e., it partially accommodates the ferroelectric instability and at the same time renders positive two of the imaginary branches. The fact that there still remains one imaginary branch, and that the dielectric constant is still not positive, implies that there is yet another distortion required to stabilize the model structure. No other significant distortions were detected from the PDF analysis of the real crystal and indeed the O_z distortion was seen to be smaller in magnitude. The ionic approximation used in the modeling is acceptable in this system but may lead to an overestimate of the ferroelectric behavior since in the real crystal, there is a degree of covalency at least in the CuO_2 plane. If this is the case, then it may be possible to stabilize the real structure with a smaller displacement of oxygen along z and no additional distortions. In this case, the driving force for the distortion would be a ferroelectric instability.

The calculation also indicated that the elastic constants for tensile stretches along the x/y and z directions become smaller on introduction of the distortion. The effect is large: c_{11} is almost halved and c_{33} is also reduced by almost one-third. We should also note that the calculations found a large compressive stress along the z direction. The presence of such a lattice pressure acting to squeeze the planes is of interest as such a pressure is known to enhance the superconducting effect in Y 1:2:3, (Ref. 2) and La 2:1:4,⁴² if not all of the cuprate superconductors.

It is possible that the strontium has a role in preventing the pressure from relaxing, thus allowing the planes to distort, making the lattice energy more negative, without the structure transforming to a completely new one. The ionic radius of strontium ion is too large for this site, which has two effects. First it reduces the

squeezing of the a/b lattice parameter, which the calculation indicates would accompany a relaxation of lattice pressure. Furthermore, it lowers the driving force for such a change by interrupting the O_z displacements. Close to the strontium ion we might expect all of the oxygen ions to be displaced outward from the cell rather than regularly up and down from the plane. In this way strontium ions distributed regularly through the matrix would disrupt the periodicity of the observed distortion and would tend to reduce the magnitude of the O_z displacements. Both of these results are in accordance with experimental observation and would suggest that the lattice pressure, as calculated by the simulation, is an overestimate, depending as it does on periodically repeating displacements of magnitude 0.3 Å instead of the short-range displacements of magnitude 0.1 Å as seen in the experiment. Thus, the predictions of the calculation of a lattice pressure and lower elastic constants appear to be consistent with observation when the presence of stabilizing strontium ions is considered.

The calculation indicates that, in the ionic approximation, the structure is more stable with the displacements of oxygen than when it contains truly planar CuO_2 sheets, in accordance with the observed behavior of the real material. It appears that there is no strong restoring force holding the oxygen in the plane. Thus, relatively small perturbing forces are able significantly to affect the local structure of the planes.

VII. CONCLUSION

We have presented evidence that a real static, or quasi-static, distortion is occurring to the CuO_2 planes in $Ca_{0.85}Sr_{0.15}CuO_2$. This distortion is characterized as being a displacement of oxygen perpendicular to the plane, of between 0.08 and 0.12 Å, which may be random from site to site but is more likely to be correlated. A possible model for the correlations, consistent with experiment, has been presented.

The importance of this deviation from planarity of the ideal planes comes from the consequences this would have for high- T_c superconductivity. The first point to

note is that locally the symmetry may not be the same as the overall average symmetry. This would be the case, for instance, if a short-range, orthorhombic, correlated structure exists, as in the proposed model, although on average the crystal symmetry remains tetragonal. Of more direct importance is the fact that the point symmetry of the ionic sites will be different in the presence of a distortion. In the proposed model the oxygen site symmetry would be reduced from mmm to 2.

The importance of ionic bonding is apparent though it is clear that this is insufficient to explain the detailed properties of the plane. The geometry of the ionic arrangements, however, is such that the interatomic forces do little to restrain oxygen in the plane, and it would appear that only a small driving force is needed significantly to affect the structure of the planes. This is true of all the categories of planes outlined in the discussion and it is not surprising that, even in apparently simple structures, these planes behave in a complex way. Indeed, in the model compound $Ca_{0.85}Sr_{0.15}CuO_2$, there is no driving force from external elements in the structure. However, our evidence suggests that the planes are distorted due to an intrinsic driving force. These considerations are of special relevance in the superconducting materials since it appears that the carrier holes present in these reside on the in-plane oxygen ions.

ACKNOWLEDGMENTS

The authors are grateful to B.H. Toby for help in collecting data and in its analysis, and W. Dmowski for useful discussions. Thanks also go to David Price, C.-K. Loong, and D. LePoire for their help in collecting inelastic neutron data. We would also like to thank R. G. Bell for help with the simulation studies. Work at the University of Pennsylvania was supported by the National Science Foundation Materials Research Laboratory (MRL) program through Grant Nos. DMR-8819885 and DMR-881027. The Intense Pulsed Neutron Source is operated as a user facility by the U.S. Department of Energy, Division of Materials Sciences, under Contract No. W-31-109-Eng-38.

¹J. G. Bednorz and K. A. Müller, Z. Phys. B **64**, 189 (1986).

²M. K. Wu, J. R. Ashburn, C. J. Torng, P. H. Hor, R. L. Meng, L. Gao, Z. J. Huang, Y. Q. Wang, and C. W. Chu, Phys. Rev. Lett. **58**, 908 (1987).

³H. Maeda, Y. Tanaka, M. Fukutomi, and T. Asano, Jpn. J. Appl. Phys. Lett. **4**, L209 (1988).

⁴C. W. Chu, J. Bechtold, L. Gao, P. H. Hor, Z. J. Huang, R. L. Meng, Y. Y. Sun, Y. Q. Wang, and Y. Y. Xue, Phys. Rev. Lett. **60**, 941 (1988).

⁵Z. Z. Sheng, A. M. Hermann, A. El Ali, C. Almasan, J. Ware, T. Datta, and R. J. Matson, Phys. Rev. Lett. **60**, 937 (1988).

⁶J. Yu, A. J. Freeman, and J.-H. Xu, Phys. Rev. Lett. **58**, 1035 (1987).

⁷V. B. Grande, Hk. Müller-Buschbaum and M. Schweizer, Z. Anorg. Allg. Chem. **428**, 120 (1977).

⁸C. C. Torardi, M. A. Subramanian, J. C. Calabrese, J.

Gopalakrishnan, K. J. Morrissey, T. R. Askew, R. B. Flippen, U. Chowdhury, and A. W. Sleight, Phys. Rev. B **38**, 225 (1988).

⁹M. A. Subramanian, C. C. Torardi, J. Gopalakrishnan, P. L. Gai, J. C. Calabrese, T. R. Askew, R. B. Flippen, and A. W. Sleight, Science **242**, 249 (1988).

¹⁰T. Siegrist, S. Sunshine, D. W. Murphy, R. J. Cava, and S. M. Zahurak, Phys. Rev. B **35**, 7137 (1987).

¹¹J. J. Capponi, C. Chaillet, A. W. Hewat, P. Lejay, M. Marezio, N. Nguyen, B. Raveau, J. L. Soubeyrou, J. L. Thoulence, and R. Tournier, Europhys. Lett **3**, 1301 (1987).

¹²M. A. Subramanian, J. C. Calabrese, C. C. Torardi, J. Gopalakrishnan, T. R. Askew, R. B. Flippen, K. J. Morrissey, U. Chowdhury, and A. W. Sleight, Science **239**, 1015 (1988).

¹³T. Siegrist, S. M. Zahurak, D. W. Murphy, and R. S. Roth,

- Nature **334**, 231 (1988).
- ¹⁴J. D. Jorgensen, H.-B. Schüttler, D. G. Hinks, D. W. Capone II, K. Zhang, M. B. Brodsky, and D. J. Scalapino, Phys. Rev. Lett. **58**, 1024 (1987).
- ¹⁵A. Williams, G. H. Kwei, R. B. Von Dreele, A. C. Larson, I. C. Raistrick, and D. L. Bish, Phys. Rev. B **37**, 7960 (1988).
- ¹⁶G. J. McIntyre, A. Renault, and G. Colin, Phys. Rev. B **37**, 5148 (1987).
- ¹⁷M. A. Beno, L. Soderholm, D. W. Capone, II, D. G. Hinks, J. G. Jorgensen, J. D. Grace, I. K. Schuller, C. U. Segre, and K. Zhang, Appl. Phys. Lett. **51**, 57 (1987).
- ¹⁸W. Dmowski, B. H. Toby, T. Egami, M. A. Subramanian, J. Gopalakrishnan, and A. W. Sleight, Phys. Rev. Lett. **61**, 2608 (1988).
- ¹⁹B. H. Toby, T. E. Egami, J. D. Jorgensen, and M. A. Subramanian, Phys. Rev. Lett. **64**, 2414 (1990).
- ²⁰T. Egami, W. Dmowski, J. D. Jorgensen, D. G. Hinks, D. W. Capone, II, C. U. Segre, and K. Zhang, Rev. Solid State Sci. **1**, 101 (1987).
- ²¹R. S. Roth, C. J. Rawn, J. J. Ritter, and B. P. Burton, J. Am. Ceram. Soc. **72**, 1545 (1989).
- ²²D. Vaknin, E. Caignol, P. K. Davies, J. E. Fischer, D. C. Johnston, and D. P. Goshorn, Phys. Rev. B **39**, 9122 (1989).
- ²³M. Takano, Y. Takeda, H. Okado, M. Miyamoto, and T. Kusaka, Physica C **159**, 375 (1989).
- ²⁴T. Egami, Mater. Trans. JIM **31**, 163 (1990).
- ²⁵G. Placzek, Phys. Rev. **86**, 377 (1952).
- ²⁶B. H. Toby and T. Egami (unpublished).
- ²⁷J. D. Jorgensen, J. Faber, J. M. Carpenter, R. K. Crawford, J. R. Haumann, R. L. Hitterman, R. Lkeb, G. E. Ostrowski, R. J. Rotella, and T. G. Worlton, J. Appl. Cryst. **22**, 321 (1988).
- ²⁸R. B. VonDreele, J. D. Jorgensen, and C. G. Windsor, J. Appl. Crystallogr. **15**, 581 (1982).
- ²⁹B. G. Dick and A. W. Overhauser, Phys. Rev. **112**, 90 (1958).
- ³⁰V. Butler, C. R. A. Catlow, B. E. F. Fender, and J. H. Harding, Solid State Ion. **8**, 10 (1983).
- ³¹M. S. Islam, M. Leslie, S. M. Tomlinson, and C. R. A. Catlow, J. Phys. C **21**, L109 (1988).
- ³²C. R. Catlow, C. R. A., C. M. Freeman, M. S. Islam, R. A. Jackson, M. Leslie, and S. M. Tomlinson, Philos. Mag. A **58**, 123 (1988).
- ³³M. J. Sanders, M. Leslie, and C. R. A. Catlow, J. Chem. Soc. Chem. Commun. 1271 (1984).
- ³⁴C. W. Burnham, Am. Mineral. **75**, 443 (1990).
- ³⁵R. A. Jackson and C. R. A. Catlow, Mol. Simulation **1**, 207 (1988).
- ³⁶B. Vessal, M. Leslie, and C. R. A. Catlow, Mol. Simulation **3**, 123 (1989).
- ³⁷N. F. Mott and M. J. Littleton, Trans. Faraday Soc. **34**, 485 (1938).
- ³⁸C. R. A. Catlow, R. James, W. C. Mackrodt and R. F. Stewart, Phys. Rev. B **25**, 1006 (1982).
- ³⁹R. D. Shannon and C. T. Prewitt, Acta Crystallogr. **925**, 946 (1969).
- ⁴⁰I. D. Brown, in *Structure and Bonding in Crystals*, edited by M. O'Keefe and A. Navrotsky (Academic, New York, 1981), Vol. II.
- ⁴¹I. D. Brown, Chem. Soc. Rev. **7**, 359 (1978).
- ⁴²C. W. Chu, P. H. Hor, R. L. Meng, L. Gao, Z. J. Huang, and Y. Q. Wang, Phys. Rev. Lett. **58**, 405 (1987).